FOREX Publication
Open Access | Rapid and quality publishing

International Journal of
Electrical and Electronics Research (IJEER)
Research Article | Volume 12, Issue 3 | Pages 981-990 | e-ISSN: 2347-470X

Conversion of an Existing 3 – Phase BLDC Hub motor to a 6 – Phase BLDC Hub Motor and their Performance Analysis for EV Application

Mahesh Gaddam[1], Chakravarthy Muktevi[2] and Mangu B[3*]
[1,3]Osmania University, Hyderabad, Telangana, India; mahesh.gaddam@staff.vce.ac.in[1] , bmanguou@gmail.com[3]
[2]Vasavi College of Engineering, Hyderabad, Telangana, India; hodeee@staff.vce.ac.in

***Correspondence:** Mahesh Gaddam; *mahesh.gaddam@staff.vce.ac.in*

ABSTRACT- In this research work a six–phase BLDC Hub motor designed, developed by using an existing 3–phase BLDC Hub motor material. This conversion orients towards design modifications in the stator winding layout, the number of phases, the number of hall-sensors, placement of hall-sensors and stator winding commutation. Also, a new controller is designed to commutate the six-phase stator winding. The rotor is kept the same without any modification in geometry and number of magnets. The existing 3–phase BLDC Hub motor, which is used in two – wheel EV application, has 48 slots and 52 magnets and a concentrated double layer winding layout is observed in it. This paper presents a novel direct approach for the conversion of the existing 3–phase BLDC Hub motor to a six–phase BLDC Hub motor. Using this proposed approach, a six-phase winding layout is designed and developed for the existing 48 slots stator of the BLDC Hub motor. This approach reduces the number of iterations to determine the proper phase sequence and phase offset among the phase windings compared to regular Cros' method. In this work, first the existing 3–phase BLDC Hub motor is dismantled, and its stator is rewound with the six – phase winding layout, which is determined by author's presented direct approach. The winding was designed in such a way to keep the stator slot fill factor in practical limits. Six hall-sensors placed in the stator slots to identify the position of the rotor. Secondly, a new controller is designed to run the developed six-phase BLDC Hub motor. Six-phase and 3–phase BLDC Hub motors are loaded at common load conditions, for performance comparison, and experimental results of both the motors presented. The results show that the six-phase BLDC Hub motor performs better than the existing 3–phase BLDC Hub motor. Hence, this work proves that the conversion of existing 3–phase BLDC Hub motor to a six–phase BLDC Hub motor is viable and can be adopted commercially.

Keywords: BLDC motor; Concentrated winding; Design of BLDC; Hub motor; Six–phase winding.

ARTICLE INFORMATION
Author(s): Mahesh Gaddam, Chakravarthy Muktevi and Mangu B;
Received: 17/07/2024; **Accepted**: 13/08/2024; **Published**: 20/08/2024;
e-ISSN: 2347-470X;
Paper Id: IJEER 1707-18;
Citation: 10.37391/ijeer.120332
Webpage-link:
https://ijeer.forexjournal.co.in/archive/volume-12/ijeer-120332.html

crossref member CROSSREF.ORG THE CITATION LINKING BACKBONE

Publisher's Note: FOREX Publication stays neutral with regard to Jurisdictional claims in Published maps and institutional affiliations.

1. INTRODUCTION

In India, electric scooters use is gaining more popularity for individual local transportation in urban and sub-urban areas due to its low running cost per kilometre. Apart from running cost, they do not pollute the atmosphere and silence when compared with IC engine scooters. In an electric scooter the main components are the drive motor, battery, the controller, and battery charger apart from other auxiliary electrical and mechanical components [1, 2]. While designing an electric scooter the first and foremost component to be accounted for is an electric motor. Therefore, the electric motor used must be able to produce adequate output power for the propulsion of the vehicle for a given load condition and the speed. The important task is to determine an appropriate type and ratings of a motor based on the required performance of the scooter. A Brushless DC motor of out-runner topology, also known as the BLDC Hub motor, is considered due to its more efficiency and reliability [3 – 7] compared to the regular motors. The out-runner topology drops the use of drive belt or gear wheels or pulleys as the rotor is directly welded to the rim of the rear wheel tire. This reduces the power loss while transmitting power to tire and increases efficiency [5]. The BLDC Hub motors used in EV applications are also due to their good torque-speed characteristics, low noise level, and simple design [7, 8]. In these Hub motors, all teeth concentrated winding layouts are observed popularly and compared to traditional distributed double layer windings, all teeth concentrated winding layouts have significantly reduced overhang portion [9] resulting in compact coil size [10] and lowered copper consumption [11, 12]. The Brushless DC Hub motors have smaller axial length and a larger diameter of the stator, which gives lesser active coil side length [13]. Manufacturing of these Hub motors is simple and cost saving as the consumption of lamination material and copper is lower [14]. A concentrated winding Brushless DC Hub motor performance relays on the slot-pole count [15, 17] and hence it must be chosen wisely. For low-speed direct drive EV applications, concentrated all teeth winding layouts usually have SPP in the range of 0.25 – 0.5 [16]. The Brushless DC Hub motors have fractional slots per pole per phase, causing lower alignment among the stator teeth and the rotor pole, resulting in lesser cogging torque [18]. The

Brushless DC Hub motors are of out-runner topology, have their own limitations and In-runner topology BLDC motors suitable for high-speed applications [19, 20]. A significant challenge for current L1 class standard electric scooters is their comparatively low gradeability when measured against their internal combustion engine-driven counterparts. Consequently, electric scooters often have difficulty ascending ramps in elevated areas, as well as in underground or cellar parking locations. This limitation can result in discomfort for the rider(s) and may potentially lead to hazardous situations during ascent. This work also motivated with the approach of VARCAS; a Hyderabad (India) based automobile pvt. Ltd company. The company makes Electric scooters with Brushless DC Hub motor imported from China. The company wanted the authors to design and develop the Brushless DC Hub motor locally with some improvements in its performance and reliability.

2. SPECIFICATIONS AND METHODOLOGY

The approach of VARCAS has set off the work of a Six-phase BLDC Hub motor. The existing 3–phase BLDC Hub motor specifications are given in *table 1*. This BLDC Hub motor is dismantled, and its stator is rewound with the six – phase winding layout, which is determined by author's presented direct approach. The complete assembly of the Hub motor is shown in *figure 1*.

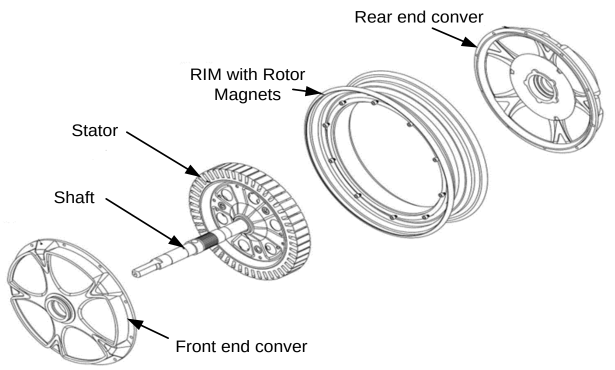

Figure 1. Assembly of BLDC Hub motor

Table 1. Specifications of existing 3-phase BLDC Hub motor

Parameeter	Value
Rated Out Put Power	850 W
Rated Speed	550 r.p.m
Rated Torque	15 N-m
Rotor Outer Dia	230 mm
Rotor Inner Dia	210 mm
Rotor Stacking length	30 mm
Stator Outer Dia	208 mm
Stator Inner Dia	163 mm
Stator Stacking length	29 mm
Magnet Size (L x W x T)	30 x 12.5 x 2.5 mm

This 48slot-52magnet count gives a winding factor of 0.9494 for 3-phase winding layout [15, 21] and 0.9801 for 6-phase winding layout. A winding factor value greater than 0.94 gives better performance of the motor as the performance is influenced by the winding factor.

2.1. Proposed method for winding design

The following assumptions are made while designing a six-phase balanced concentrated double layer winding layout to the existing 48 slots stator:

1. The number of slots (N_s) should be multiple of the number of phases (N_{ph}).
2. There are no empty slots in the stator.
3. Two coil sides are placed in each slot.
4. A slot – pole count must allow the winding layout to get back EMF magnitudes equal in all phases and 60 ^{0}E off set from each other are considered.
5. The number of turns in all the coils and span is the same.

The above assumptions give a winding layout capable of high performance and easy to wound. The coil span (CS) should be close to 180 ^{0}E and is determined by

$$CS = \max(\text{fix}(N_s / N_m), 1) \quad (1)$$

The stator slot angle (θ_{sl}) relative to the first stator slot can be used to determine phase difference.

$$\theta_{sl} = (S\text{-}1)(N_m / N_s)180\ ^0E \quad (2)$$

Where '*S'* is the slot number. These angles may extend outside the range $-180^0 E \leq \theta \leq 180\ ^0E$. A reminder function is used to determine the principal angle related to each of these angles.

$$\theta_{sl} = \text{rem}\ \{(S\ \text{-}1)(N_m / N_s)180\ ^0E,\ 360^0 E\} \quad (3)$$

Equation (3) modified such that it avoids use of the rem function and gives the number of slots for phase offset by the following equation.

$$M_o = (0.5 + 2q)(2N_s/3N_m) \quad (4)$$

Where q is an integer. While laying out a winding, coils with a span of 'S' are placed in slots such that relative angular coil midpoints are as close to 0^0 E and 180^0 E apart. Coils close to 0^0 E are wound in one direction and the coils close to 180^0 E are wound in the reverse direction since the magnetic flux direction reverses at 180^0 E. The coil locations must be chosen that are as close as possible to 0^0 E and 180^0 E separation. The number of coils per phase is given by

$$N_{cph} = N_s/N_{ph} \quad (5)$$

For the existing 48 slots and 52 poles Hub motor, the nominal coil span CS = 1, the Slot angle $\theta_{sl} = 195^0$ E i.e. Each coil offset angle is 195^0 E w.r.t the consecutive coil. The phase offset M_o = 4 slots and the coils per phase are 8. The total number of coils in the stator is equal to 48. Each coil offset angle and associated *In* and *Out* slots are listed in *table 2*. These coils offset angles are valid and may extend outside the range $-180^0 E \leq \theta \leq 180^0$

FOREX Publication
Open Access | Rapid and quality publishing
International Journal of Electrical and Electronics Research (IJEER)
Research Article | Volume 12, Issue 3 | Pages 981-990 | e-ISSN: 2347-470X

E. The principal angle (θ) related to each of these angles is determined by

$$\theta = \text{rem}\,(\theta + 180^0, 360^0) \qquad (6)$$

Table 3 provides the angle (θ) of each coil with respect to the first coil. The coil's winding direction is modified (inter change of *In* slot & *Out* slot) whose angle (θ) is greater than 90^0 E and their corresponding angle by 180^0 E. This gives the prospective coils for phase A. Table 4 shows the details along with *In* and *Out* slots. Eight coils should be selected from *table 4* to lay a winding for phase A. Coils, which are close to 0^0 E should be used and its angular spread of the winding should be minimum. Since eight coils are required per phase, the coils numbered 1, 2, 3, 4, 25, 26, 27, and 28 are closest to 0^0 E and have a total spread of 45^0 E are chosen. *Table 5* shows the phase A winding layout. Since the phase offset of M_o = 4 slots lead to an angle 60^0 E offset between phases A and D, hence each coil in phase D is shifted by 4 slots with respect to the corresponding coil in phase A.

Table 2. Each Coil offset angle and it's associated *In* & *Out* slots

Coil No	1	2	3	4	5	6	7	8	9	10	11	12
Coil Angle	0	195	390	585	780	975	1170	1365	1560	1755	1950	2145
In Slot	1	2	3	4	5	6	7	8	9	10	11	12
Out Slot	2	3	4	5	6	7	8	9	10	11	12	13
Coil No	13	14	15	16	17	18	19	20	21	22	23	24
Coil Angle	2340	2535	2730	2925	3120	3315	3510	3705	3900	4095	4290	4485
In Slot	13	14	15	16	17	18	19	20	21	22	23	24
Out Slot	14	15	16	17	18	19	20	21	22	23	24	25
Coil No	25	26	27	28	29	30	31	32	33	34	35	36
Coil Angle	4680	4875	5070	5265	5460	5655	5850	6045	6240	6435	6630	6825
In Slot	25	26	27	28	29	30	31	32	33	34	35	36
Out Slot	26	27	28	29	30	31	32	33	34	35	36	37
Coil No	37	38	39	40	41	42	43	44	45	46	47	48
Coil Angle	7020	7215	7410	7605	7800	7995	8190	8385	8580	8775	8970	9165
In Slot	37	38	39	40	41	42	43	44	45	46	47	48
Out Slot	38	39	40	41	42	43	44	45	46	47	48	1

Selecting coils numbered 5, 6, 7, 8, 29, 30, 31, and 32 from *table 4* to form the phase D winding coils and its layout as shown in *table 6*. Keeping phase offset of 60^0 E (4 slots) w.r.t the phase D coils, phase B coils can be placed in the slots. Selecting coils numbered 9, 10, 11, 12, 33, 34, 35, and 36 gives the phase B winding coils. Similarly, phases E, C and F coils are placed in the slots keeping phase offset of 60^0 E with respect to each phase and choosing the coils close to 0^0 E. *Table 7* shows Six – phase double layer concentrated winding layout designed for the existing 48 slots, 52 poles Hub motor using the proposed direct approach method. This Six – phase winding layout developed is depicted in *figure 2*. A 15 strands copper conductor used in the winding and each strand gauge is 25SWG. There are 6 turns in each coil of phase. The winding was designed in such a way to keep the stator slot fill factor in practical limits [22].

Table 3. The principal angle of each coil with respect to the first coil and it's associated *In* & *Out* slots

Coil No	1	2	3	4	5	6	7	8	9	10	11	12
Principle Angle	0	-165	30	-135	60	-105	90	-75	120	-45	150	-15
In Slot	1	2	3	4	5	6	7	8	9	10	11	12
Out Slot	2	3	4	5	6	7	8	9	10	11	12	13
Coil No	13	14	15	16	17	18	19	20	21	22	23	24
Principle Angle	-180	15	-150	45	-120	75	-90	105	-60	135	-30	165
In Slot	13	14	15	16	17	18	19	20	21	22	23	24
Out Slot	14	15	16	17	18	19	20	21	22	23	24	25
Coil No	25	26	27	28	29	30	31	32	33	34	35	36
Principle Angle	0	-165	30	-135	60	-105	90	-75	120	-45	150	-15
In Slot	25	26	27	28	29	30	31	32	33	34	35	36
Out Slot	26	27	28	29	30	31	32	33	34	35	36	37
Coil No	37	38	39	40	41	42	43	44	45	46	47	48
Principle Angle	-180	15	-150	45	-120	75	-90	105	-60	135	-30	165
In Slot	37	38	39	40	41	42	43	44	45	46	47	48
Out Slot	38	39	40	41	42	43	44	45	46	47	48	1

FOREX Publication
Open Access | Rapid and quality publishing

International Journal of
Electrical and Electronics Research (IJEER)
Research Article | Volume 12, Issue 3 | Pages 981-990 | e-ISSN: 2347-470X

Table 4. Changed winding direction of coils whose principal angle > 90^0 E and it's associated *In* & *Out* slots

Coil No	1	2	3	4	5	6	7	8	9	10	11	12
Principle Angle	0	15	30	45	60	75	90	-75	-60	-45	-30	-15
In Slot	1	3	3	5	5	7	7	8	10	10	12	12
Out Slot	2	2	4	4	6	6	8	9	9	11	11	13
Coil No	13	14	15	16	17	18	19	20	21	22	23	24
Principle Angle	0	15	30	45	60	75	-90	-75	-60	-45	-30	-15
In Slot	14	14	16	16	18	18	19	21	21	23	23	25
Out Slot	13	15	15	17	17	19	20	20	22	22	24	24
Coil No	25	26	27	28	29	30	31	32	33	34	35	36
Principle Angle	0	15	30	45	60	75	90	-75	-60	-45	-30	-15
In Slot	25	27	27	29	29	31	31	32	34	34	36	36
Out Slot	26	26	28	28	30	30	32	33	33	35	35	37
Coil No	37	38	39	40	41	42	43	44	45	46	47	48
Principle Angle	0	15	30	45	60	75	-90	-75	-60	-45	-30	-15
In Slot	38	38	40	40	42	42	43	45	45	47	47	1
Out Slot	37	39	39	41	41	43	44	44	46	46	48	48

Table 5. Phase A coils with *In* & *Out* slots

Coil No	1	2	3	4	25	26	27	28
Coil Angle	0	15	30	45	0	15	30	45
In Slot	1	3	3	5	25	27	27	29
Out Slot	2	2	4	4	26	26	28	28

Table 6. Phase D coils with *In* & *Out* slots

Coil No	5	6	7	8	29	30	31	32
Coil Angle	0	15	30	45	0	15	30	45
In Slot	5	7	7	9	29	31	31	33
Out Slot	6	6	8	8	30	30	32	32

(a)

(b)

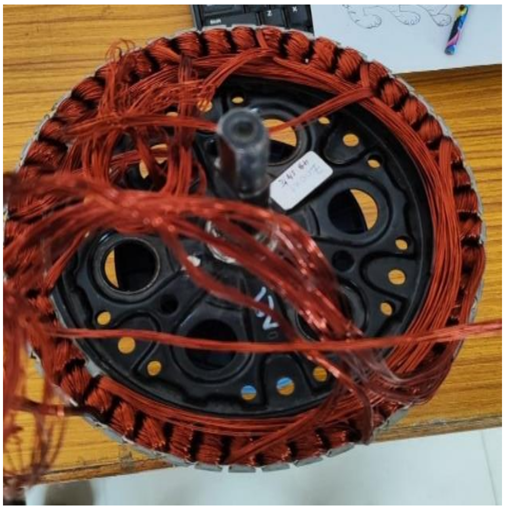

(c)

Figure 2. Winding layout (a) Winding of Phase A; (b) Winding of Phase A&D; (c) Winding of all Phases

Table 7. Six – phase winding layout of 48S – 52P Hub motor using simple approach method

Slot	Phase A	Phase D	Phase B	Phase E	Phase C	Phase F	Slot	Phase A	Phase D	Phase B	Phase E	Phase C	Phase F
1	In					In	25	In					In
2	Out, Out						26	Out, Out					
3	In, In						27	In, In					
4	Out, Out						28	Out, Out					
5	In	In					29	In	In				
6		Out, Out					30		Out, Out				
7		In, In					31		In, In				
8		Out, Out					32		Out, Out				
9		In	In				33		In	In			
10			Out, Out				34			Out, Out			
11			In, In				35			In, In			
12			Out, Out				36			Out, Out			
13			In	In			37			In	In		
14				Out, Out			38				Out, Out		
15				In, In			39				In, In		
16				Out, Out			40				Out, Out		
17				In	In		41				In	In	
18					Out, Out		42					Out, Out	
19					In, In		43					In, In	
20					Out, Out		44					Out, Out	
21					In	In	45					In	In
22						Out, Out	46						Out, Out
23						In, In	47						In, In
24						Out, Out	48						Out, Out

2.2. Placing of Hall sensors

The number of hall sensors used for BLDC hub motor is equal to the number of phases. Typically, more Hall sensors might be required to provide the necessary position feedback to handle the six phases effectively. This requires strategic placement to cover multiple phases and ensure reliable operation. Implications for the placement and utilization of Hall sensors, such as each sensor must be positioned to capture accurate rotor position data corresponding to the increased number of phases. The placement of Hall sensors must be carefully aligned to accurately detect the rotor position and facilitate the correct sequencing of the phase currents. Precise alignment of the Hall sensors becomes even more crucial with additional phases. The six hall sensors are to be placed 60^0 E apart from each other. There are two ways to place the hall sensor, one is by mounting it on a board inside the motor positioned to pick up the magnetic flux and the other is by mounting it in the stator slots. In this research work, it is proposed to place it in the stator slot. Placing of hall sensors begins with calculating the mechanical angle of each slot.

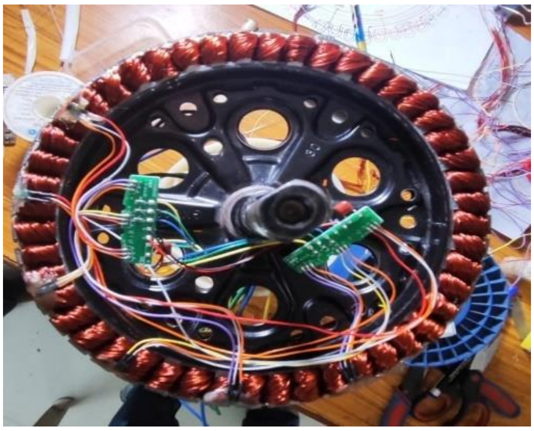

(a)

FOREX Publication
Open Access | Rapid and quality publishing
International Journal of
Electrical and Electronics Research (IJEER)
Research Article | Volume 12, Issue 3 | Pages 981-990 | e-ISSN: 2347-470X

(b)

Figure 3. Hall sensors placement (a) 6 hall sensors grouped into two sets with PCBs; (b) Final placement with packaging.

Slot mechanical angle (θ_{slm}) = (360^0M) / N_s (7)

Electrical angle of Slot (θ_{sle}) = (Nm/2) θ_{slm} (8)

The six hall sensors are to be placed 60^0 E apart from each other, by equating the equation (2) to (60 + q360) ^{0} E where q is any integer in the range 0 to [(Nm/2) -1] produces an integer result.

$$K_o = (0.5 + 2q)\,(2N_s/3N_m) \quad (9)$$

For the existing BLDC hub motor, which has N_s = 48 & N_m = 52; the q = 6 produces an integer result for K_o = 4. Hence, the spacing between each hall sensors are 4 slots that will give 60^0 E apart from each other. *Figure 3* shows the placement of Hall Sensors in the slots of the stator. Any misalignment can lead to incorrect phase switching, resulting in suboptimal motor performance, increased noise, and mechanical vibrations. Thus, meticulous calibration and testing are essential during installation.

2.3. Design of the Proposed controller

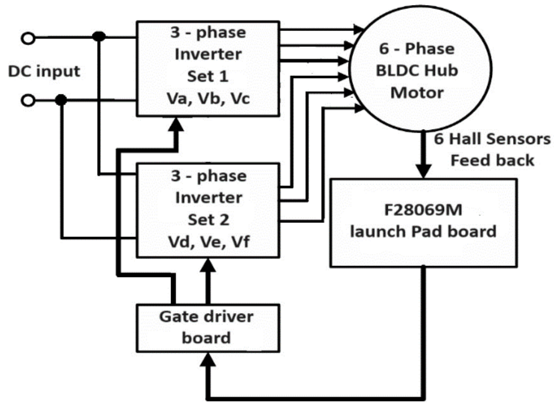

(a)

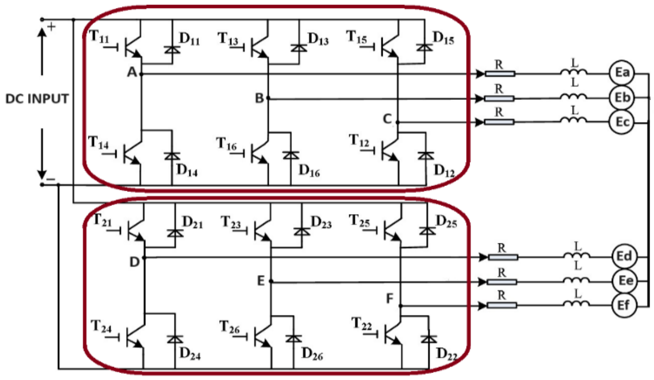

(b)

Figure 4. (**a**) Block diagram of 6-phase BLDC Hub motor; (**b**) Circuit diagram of the 6-phase windings excited with two inverter sets.

The block diagram of the closed loop control system of developed Six-phase BLDC Hub motor and circuit diagram of stator winding excitation with two inverter sets is shown in *figure 4*. Launchpad F28069M Piccolo™, a specific model of a development board of Texas Instruments™ is used to generate the PWM pulses to two Inverter sets with the help of feedback signals of hall sensors. This control board is equipped with a TMS320F28069M 32-bit MCU featuring 90 MHz C28x CPU, 256 KB Flash, 12-bit ADC, 2 encoder interfaces (eQEP) and 16 PWM pins.

Table 8. Three – phase Inverter Set1 and Set2 switching logic

θr	H_a	H_b	H_c	T 11	T 13	T 15	T 14	T 16	T 12	H_d	H_e	H_f	T 21	T 23	T 25	T 24	T 26	T 22
0^0 - 60^0	1	0	1	1	0	0	0	1	0	0	0	1	0	0	1	0	1	0
60^0 - 120^0	1	0	0	1	0	0	0	0	1	1	0	1	1	0	0	0	1	0
120^0 - 180^0	1	1	0	0	1	0	0	0	1	1	0	0	1	0	0	0	0	1
180^0 - 240^0	0	1	0	0	1	0	1	0	0	1	1	0	0	1	0	0	0	1
240^0 - 300^0	0	1	1	0	0	1	1	0	0	0	1	0	0	1	0	1	0	0
300^0 - 360^0	0	0	1	0	0	1	0	1	0	0	1	1	0	0	1	1	0	0

The switching control logic to generate PWM pulses to the two sets of 3 – phase Inverters is shown in *table 8*. The developed logic implemented by programming a TI C2000™ based MCU platform through the MATLAB Simulink.

2.4. Development of hardware system

The Six – phase winding of BLDC Hub motor is grouped into two sets of Three – phase and the six Hall sensors grouped into

Research Article | Volume 12, Issue 3 | Pages 981-990 | e-ISSN: 2347-470X

two sets, since two 3-phase inverter sets are used to supply the stator of the six-phase BLDC Hub motor. The phase offset between the two inverters on each leg is maintained at 60^0 E through the gate switching pulses of corresponding legs. The hardware setup of inverters, a gate driver board, F28069 Controller, and six-phase hub motor are shown in *figure 5*. Increasing the number of winding phases from three to six in BLDC Hub motor has certain implications for the inverter system used to drive the motor. Such as the commutation control becomes complex as each phase needs precise timing for switching. The control algorithm for the inverter becomes sophisticated, inverter requires more electronic components than its three-phase counterpart, including additional power switches, gate drivers, and potentially more complex digital signal processing capabilities. This increase in components can lead to a rise in the overall cost and size of the inverter system. But the shift to a six-phase offers notable benefits in terms of performance, reliability, and efficiency. These advantages can make the transition appealing for applications demanding high-performance and robust electric motor solutions.

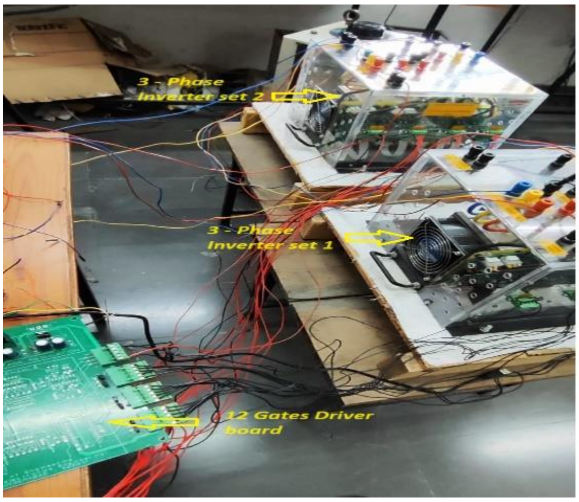

(a)

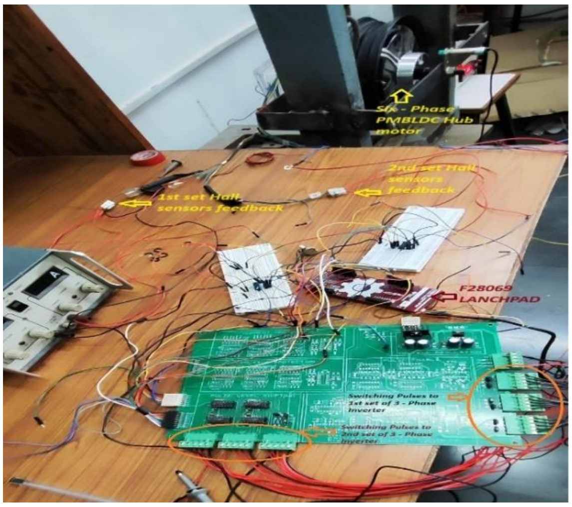

(b)

Figure 5. (a) Hardware setup of two 3 – phase Inverters sets with Gate driver board; (b) Six-phase Hub motor with Hall sensors feedback and F28069 Controller.

3. RESULTS AND DISCUSSIONS

An existing 3–phase BLDC Hub motor converted to a six–phase BLDC Hub motor. Six-phase and 3–phase BLDC Hub motors are loaded at common load conditions, for performance comparison.

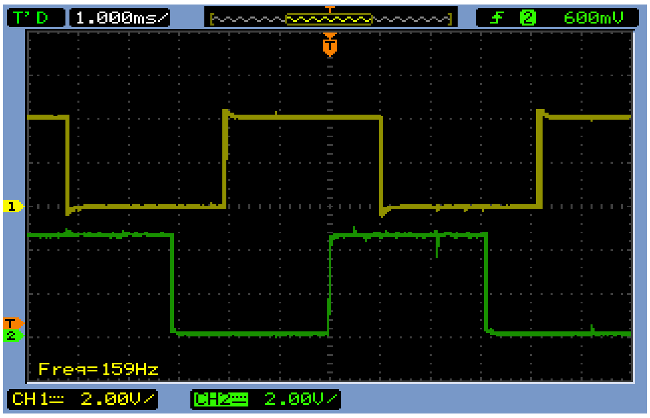

(a)

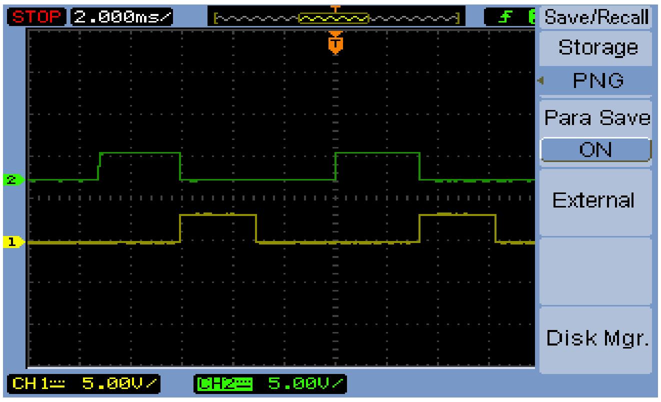

(b)

Figure 6. (**a**) Hall Sensor H_a & H_b feedback signals of set1 having 120^0 phase offset; (**b**) Gate Pulses of T_{11} & T_{13} with 120^0 phase offset

Experimental wave forms of hall sensor feedback, switching gate pulses, line voltages and current are shown through *figure 6* to *figure 7*. The experimental loading values of 3–phase and six–phase BLDC Hub motors are listed in *table 9*.

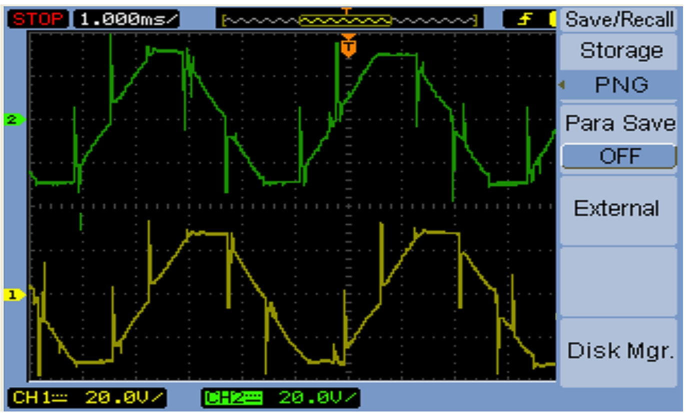

(a)

International Journal of
Electrical and Electronics Research (IJEER)
Research Article | Volume 12, Issue 3 | Pages 981-990 | e-ISSN: 2347-470X

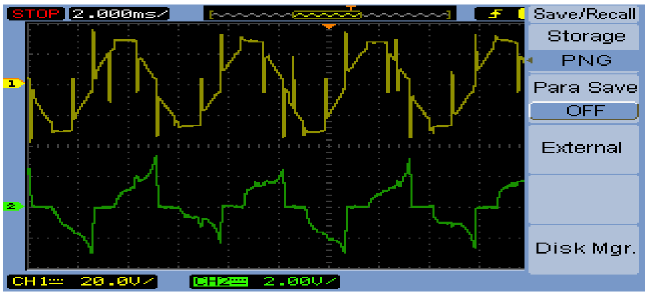

(b)

Figure 7. (a) Line Voltage VAB & VDE of Six-phase Hub motor with 600 phase difference; (b) Line voltage VAB & Current IA waveforms of Set 1 winding of Six-phase Hub motor

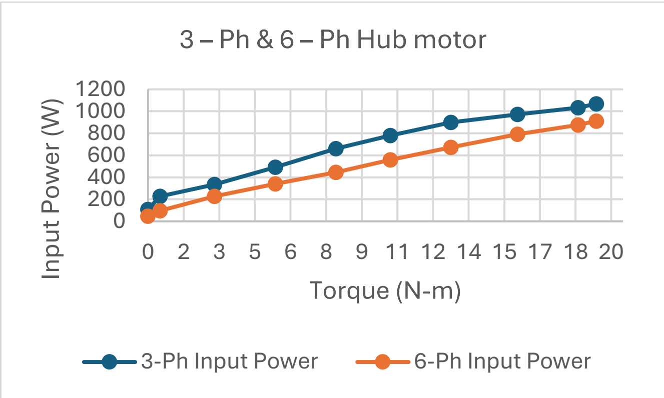

(a)

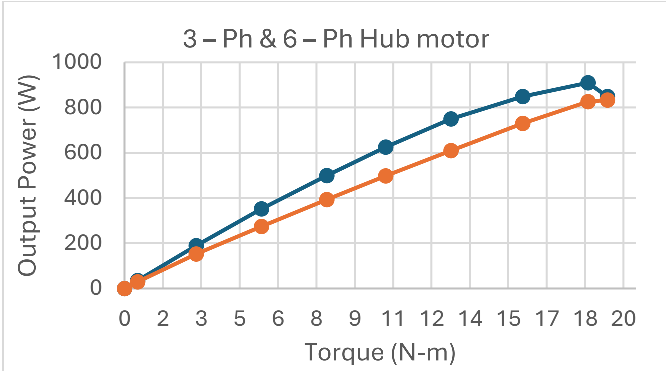

(b)

Figure 8. (a) Plot between Input power and Torque; (b) Plot between Output power and Torque

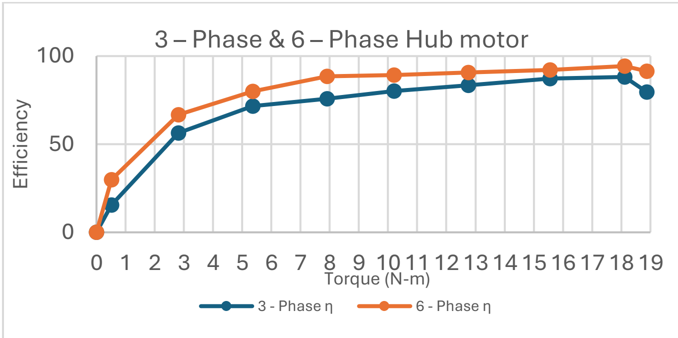

Figure 9. Plot between Efficiency and Torque

Table 9. Three – phase & Six – Phase BLDC Hub motor experimental loading summary data

S. No.	Load Torque (N-m)	3 – Ph motor Input Power (w)	6 – Ph motor Input Power (w)	3 – Ph motor Output Power (w)	6 – Ph motor Output Power (w)	3 – Ph Motor η (%)	6 – Ph motor η (%)
1	0.00	108	48	0.00	0.00	0.00	0.00
2	0.51	228	96	35.51	28.62	15.57	29.81
3	2.81	336	228	189.70	152.12	56.46	66.72
4	5.36	492	342	352.07	273.58	71.56	80.00
5	7.91	660	444	499.86	393.10	75.74	88.54
6	10.20	780	558	625.76	497.62	80.23	89.18
7	12.75	900	672	750.17	610.01	83.35	90.78
8	15.56	972	792	848.43	729.56	87.29	92.12
9	18.11	1032	876	909.81	826.41	88.16	94.34
10	18.87	1068	912	839.48	846.67	78.6	92.5

4. CONCLUSIONS

The Six – Phase concentrated the double layer winding layout was developed for existing 48 slots, 52 magnets BLDC Hub motor using the proposed direct approach method. The winding layout has a winding factor of 0.98 and the no-load cogging torque pulsations over one revolution of the rotor is 624. Cros' method does not indicate phase offset and angular spread of coils around the slots of the stator periphery is unsymmetric even though the number of coils in a phase is an even number. Whereas in the proposed method phase offset is clearly indicated and it is symmetric with minimum angular spread. The proposed six-phase winding layout produces balanced dynamic radial forces on the rotor resulting in less vibration and noise. Hence the presented direct approach is a good choice for determining the winding layout for conversion. It is also valid for other poly – phase winding layouts of more than three – phases. Six-phase and 3–phase BLDC Hub motors are loaded at common load conditions, for performance comparison, and experimental results of both the motors presented. The results show that, at the rated output power of about 850W, the 3 – Phase Hub motor produced 15.56 N-m torque whereas the 6 – Phase Hub motor produced 18.87 N-m. Thus, an increase of 21.7% of torque is obtained in the proposed Six – phase BLDC Hub motor than the three phase BLDC motor Hub of same volume. Hence, the electric vehicle using a six–phase BLDC Hub motor can climb steeper upgradient than a vehicle using 3-phase BLDC Hub motor. The efficiency of 3 – Phase Hub motor is 87.29% whereas 6 – Phase Hub motor is 92.5% at the rated power output. The six-phase BLDC Hub motor performs better than the existing 3–phase BLDC Hub motor. Hence, this work proves that the conversion of existing 3–phase BLDC Hub motor to a six–phase BLDC Hub motor is viable and can be adopted commercially. The six-phase BLDC motor can deliver higher torque and efficiency, which directly translates into improved vehicle performance and longer driving ranges. This advantage is a substantial selling point for EV manufacturers aiming to differentiate their products in a competitive marketplace. Additionally, the improved efficiency can lead to reduced energy consumption, potentially lowering operational costs over the vehicle's lifespan, which enhances the economic appeal to both manufacturers and consumers. The future works that are to be carried out are (i) The fault tolerant capability of the proposed Six - phase BLDC Hub motor has to be examined. (ii) Thermal efficiency of the motor must be analyzed and improved due to high coil packing density.

Author Contributions: In this research article, author's individual contributions specified. The "Conceptualization, supervision, Dr. M. Chakravarthy; project administration, validation, Dr.B.Mangu; methodology, software, formal analysis, investigation, resources, data curation, writing—original draft preparation, writing—review and editing, visualization, G. Mahesh. All authors have read and agreed to publish this version of the manuscript".

Funding: "This research received external funding from the management of Vasavi College of Engineering with a grant of seed money Rs. 75,000/- (Indian Rupees)".

Acknowledgments: Authors thank the management of Vasavi for their support in providing funding and also thank our colleague Dr. Bishnu Prasad Muni [Retired R & D BHEL] who provided insight and expertise that greatly assisted the research work.

Conflicts of Interest: "The authors declare no conflict of interest. This manuscript has not been submitted to, nor is under review at, another journal or other publishing venue. The authors have no affiliation with any organization with a direct or indirect financial interest in the subject matter discussed in the manuscript."

REFERENCES

[1] Amir Ahmed. Propulsion System Design and Sizing of an Electric Vehicle. International Journal of Electronics and Electrical Engineering, 2015, vol 3(1), pp. 19 - 27.

[2] Bekheira T. A Power Presizing Methodology for Electric Vehicle Traction Motor. International Review on Modelling and Simulations, 2013, vol 6 (1), pp. 29 – 32.

[3] D. Hanselman. Brushless Permanent-Magnet Motor Design, 2nd ed.; Magna Physics, Ohio 1994.

[4] R.Hendershot Jr.; TJE Miller. Design of Brushless Permanent-Magnet Motor. Magna Physics & Clarendon Press, Ohio 1994.

[5] Song B. M.; Chang K. C. Design of an Outer-Rotor Type Permanent Magnet Motor for Electric Scooter Propulsion Systems, In 2010 International Power Electronics Conference (IPEC), vol. 12, pp. 2763-2742. IEEE (2010).

[6] Anqing He; Chenxi Zhou. Evaluation of Fractional Slot Concentrated Winding Permanent Magnet Synchronous Machine for Electric Vehicle Application, IEEE International Electric Machines & Drives Conference (IEMDC), May 2019, DOI: 10.1109/IEMDC.2019.8785223.

[7] Chang-liang Xia; PERMANENT MAGNET BRUSHLESS DC MOTOR DRIVES AND CONTROLS", P.R. Tianjin University, China, ISBN:9781118188330.

[8] Y.B. Adyapaka Apatya; Aries Subiantoro; Feri Yusivar. Design and Prototyping of 3-Phase BLDC Motor, International Conference on Quality in Research (QiR): International Symposium on Electrical and Computer Engineering, July, 2017, DOI:10.1109/QIR.2017.8168483.

[9] Dieter Gerling, Electrical Machines Mathematical Fundamentals of Machine Topologies, pp-449, ISBN:9783662520321.
[10] Vladimir Dimitrov, Overview of the Ways to Design an Electric Bicycle. National Conference with International Participation (ELECTRONICA), May, 2018, DOI:10.1109/ELECTRONICA.2018.8439456.

[11] Strous T. D.; Polinder H.; Ferreira J. A., Inductance calculations for PM machines with concentrated windings. IEEE International Electric Machines & Drives Conference (IEMDC), May, 2011, DOI:10.1109/IEMDC.2011.5994636.

[12] Chun Tang; Wen L. Soong; Gene S. Liew; Nesimi Ertugrul. Effect of Pole and Slot Number Changes on the Performance of a Surface PM Machine, International Conference on Electrical Machines, Sep, 2012, DOI:10.1109/ICElMach.2012.6349867.

[13] Aimeng Wang; Chunmei Wang; Soong W. L. Design and Optimization of Interior PM Machines with Distributed and Fractional-Slot Concentrated-Windings for Hybrid Electric Vehicles, IEEE Conference and Expo Transportation Electrification Asia-Pacific (ITEC Asia Pacific), Sep, 2014, DOI:10.1109/ITEC-AP.2014.6941169.

[14] Freddy Magnussen; Heinz Lendenmann. Parasitic Effects in PM Machines with Concentrated Windings, IEEE TRANSACTIONS ON INDUSTRY APPLICATIONS, vol. 43, no. 5, September/October 2007, DOI:10.1109/TIA.2007.904400.

[15] F. Libert; J. Soulard. Investigation on Pole-Slot Combinations for Permanent Magnet Machines with Concentrated Windings, Jan, 2004.

[16] Florence Meier, Permanent-Magnet Synchronous Machines with Non-Overlapping Concentrated Windings for Low-Speed Direct-Drive Applications.

[17] K. Latha Shenoy; M. Satyendra Kumar. Design Topology and Elec tromagnetic Field Analysis of Permanent Magnet Brushless DC Mo tor for Electric Scooter Application, International Conference on Elec trical, Electronics, and Optimization Techniques (ICEEOT), March 2016, DOI:10.1109/ICEEOT.2016.7754942.

[18] Zhu Z.Q.; Howe D. Influence of Design Parameters on Cogging Torque in Permanent Magnet Machines, IEEE Transactions on Energy Conversion, vol. 15, no. 4, pp. 407- 412, Dec. 2000., DOI:10.1109/60.900501.

[19] Aditya Raj, Investigations on Permanent Magnet Machines for Electric Vehicle Applications. B.Tech theses, Indian Institute of Engineering Science and Technology, Shibpur, W.B., 2019.

[20] Skaar S. E.; Krøvel O.; Nilssen R. Distribution, Coil-span and Winding Factors for PM Machines with Concentrated Windings. In proceedings of ICEM-2006, Chania (Greece), 2006.

[21] Cros J.; Viarouge P., Synthesis of high-performance pm motors with concentrated windings, IEEE Transactions on Energy Conversion, vol. 17, no. 2, pp. 248-253, Jun. 2002.

[22] Mahesh G; Chakravarthy M; Mangu B; "A Simple Approach for the Design and Development of 6 – phase winding for high slot – pole count PMBLDC Hub Motor used in EV Applications", International Journal of Intelligent Systems and Applications in Engineering, vol. 12(4), pp. 1680 – 1688.